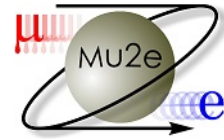




Fermilab



Mu2e Tracker's Gas Connection

Author:
Andrea FINO

Supervisor:
RA Mete YUCEL
Co-Supervisor:
Scientist Aseet MUKHERJEE

*The following report is the result of the internship at FNAL
(Batavia, Aug-Sept 2019)*

in the

Mu2e Tracker's Group

October 30, 2019

"It's better than nothing."

Smart Unknown

Abstract

This report is a resume of the activities in which I was involved during my internship at Fermilab Particle Physics and Accelerator Laboratory in Batavia.

The experiment at whom my work is connected is the Mu2e experiment, in particular I worked in the Tracker's group.

The main task of my training program was to design a gas service connection that take place in a small volume located between the Tracker and the Calorimeter (two main elements that constitute the detector).

During the initial phase I was lightly trained about the experiment and its general design, then I was supervised on my specific task.

All the work aimed to reach a design solution that could meet all the BCs, in this view, a reasonable solution was prototyped and tested.

The tests performed at Lab 3 were another fundamental aspect of my experience at Fermilab closing the circle of studying, modelling, machining and testing.

I want to thank primarily Aseet Mukherjee and Mete Yucel that were my supervisors, they constantly spent their time attempting to create a favourable workplace, suggesting, listening and meeting all the requests in short time, working for them was absolutely like "working with them", without their help achieve the result would be greatly harder. Giuseppe Gallo deserve a special thanks too for revising mostly of my work and being always available for support.

I had also the chance to share my work during the "Weekly Tracker's Meetings" dealing with other bright engineers and physicists, between them I really appreciate George Ginter, Russel Rucinski, Yujing Sun and Waqar Ahmed.

I want also to express my gratitude to Simone Donati, Giorgio Bellettini and Emanuela Barzi that make this unique experience possible organizing this program for decades.

Thanks to my Mother, my Father, my Brother, my Nephew, my uncle Damiano and my friend Simona always near, never stopping to dream with me.

Contents

Abstract	ii
1 Introduction	1
1.1 Mu2e Experiment	1
1.2 Mu2e Technical Design	1
2 Mu2e Tracker	4
2.1 Straw	4
2.2 Panel, Plane, Station	4
2.3 Frame	6
3 Problem Definition and Design Requirements	7
3.1 Problem Definition	7
3.1.1 Geometric Constraints	8
3.1.2 Working Constraints	9
4 Preliminary Design and Analyses	10
4.1 Preliminary Design and General Considerations	10
4.1.1 Printed Part	10
4.1.2 Connectors	11
4.1.3 Interfaces	11
4.1.4 Blocking System	11
4.2 Preliminary Analyses	12
5 Printed Part	14
5.1 First-phase approach	14
5.1.1 Script description	15
5.1.2 First-phase results	15
5.2 Second-phase approach	16
5.2.1 Script description	16
5.2.2 Second-phase results	17
5.3 Conclusion	18
6 Connectors	20
6.1 Preliminary design ideas	20
6.2 Actual Design	22
6.3 O-ring Study	22
6.3.1 Standard Off the Shelf	23
6.3.2 Non Standard Off the Shelf	24
6.3.3 A Brief Comparison	24
6.4 Pressure Drop Evaluation	25
6.5 Equipments	25
6.5.1 Old Equipment and Laboratory Activities	26

6.5.2	New Equipment	27
6.6	Conclusion	27
7	Interfaces	29
7.1	A Short Overview	29
8	Blocking System	30
8.1	External Structure	30
8.2	Comb	31
A	Non Standard off the shelf OR formulas	32
B	Pressure Drop Evaluation	33
C	Mechanical Drawings	35
D	Bibliography	40

List of Figures

1.1	Layout of the Mu2e facility	2
1.2	The Mu2e Detector	2
2.1	Straw	4
2.2	Panel	5
2.3	Half Plane	5
2.4	Station	6
2.5	Tracker	6
3.1	Line Scheme	7
3.2	Volume Available	8
4.1	Preliminary General Design	10
4.2	Regular Pattern	12
4.3	Worst LC scheme	13
5.1	Fundamental Cell Structures	15
5.2	MATLAB First-Phase Result.	16
5.3	MATLAB Second-Phase Result	18
5.4	SolidWorks Thickness Analysis	19
6.1	Calorimeter Side with Kynar Tubes	20
6.2	Connector: Radial Seal with Bushing	21
6.3	Connector: Tapered Sealing with Threaded Connection	21
6.4	Connector: Axial Sealing with Threaded Connection	22
6.5	Connector: 3D Model on NX	22
6.6	OR 004 AS-568: Geometry	24
6.7	Standard ORs from a Specific Vendor	25
6.8	Pressure Drop Evaluation with FLUENT	26
6.9	Old Test Equipment	26
6.10	Insert Plugged with Epoxy	27
6.11	Parts Ready for the Test	28
6.12	Equipment Mounted on the Vacuum Chamber	28
7.1	Suggestion for a Stand-alone Interface	29
8.1	External Structure Mounted on the Printed Part	30
8.2	Blocking System: How the comb hold the connectors	31
B.1	Connector: 2D Geometry	33
C.1	Insert, Mechanical Drawing	36
C.2	KF Flange Modified, Mechanical Drawing	37
C.3	Sealing Screw Modified, Mechanical Drawing	38
C.4	CF Modified, Mechanical Drawing	39

List of Tables

6.1 Standard and Non Standard OR Solutions	25
--	----

List of Abbreviations

FNAL	F ermilab N ational A ccelerator L aboratory
BC	B oundary C ondition
SES	S ingle S ensitivity E vent
IFB	I nstrument B ulkhead F eedthrough
CLFV	C harged L epton F lavor V iolation
MECO	M uon to E lectron C ONversion (Experiment)
PT	P roduction T arget
PS	P roduction S olenoid
TS	T ransport S olenoid
DS	D etector S olenoid
MST	M uon S topping T arget
DIO	D ecay I n O rbital
PAAS	P anel A ssembly (and) A lignment S ystem
SS	S tainless S teel
LC	L oad C ase
OR	O R ing
ID	I nside (hole) D iameter
CS	C ross S ection
RMS	R oot M ean S quare (surface finishing)

List of Symbols

p_{in}	inner pressure
p_{out}	outer pressure
g	gravitational acceleration
μ	muon
τ	tau
ν	neutrino
Φ	flow
ϕ	diameter
ω	speed

Chapter 1

Introduction

The knowledge of the experiment's goal is worth to clarify what's the role of the Tracker and than that of the parts designed. For this reason a brief and general explanation is made before going on with the Tracker's topic.

1.1 Mu2e Experiment

The goal of the Mu2e experiment is to observe the process $\mu^- \rightarrow e^-$. The observation of this phenomena, that is the conversion of a negative muon into an electron (in the field of a nucleus) without producing a neutrino, is an example of Charged Lepton Flavor Violation¹ and will results in a monochromatic electron with an energy of 104.97MeV, slightly below the muon's one.

Mu2e experiment is based on the MECO experiment proposed at Brookhaven, and the earlier MELC experiment of the Russian Institute for Nuclear Research, the idea is to improve[2]:

1. The Single event sensitivity (SES) of four order of magnitude and reach 3×10^{-17} on the conversion rate, and be able to set a limit of 6×10^{-17} at 90% confidence limit;
2. A 5σ discovery reach at 2×10^{-17} .

Why this experiment is so meaningful and attractive? a discovery would be an example beyond the Standard Model, this can help to deep our knowledge about most fundamental questions about matter and universe. Observing muon-to-electron conversion will also remove a hurdle to understanding why particles in the same category, or family, decay from heavy to lighter, more stable mass states[5].

1.2 Mu2e Technical Design

Mu2e will use the Fermilab Delivery Ring to create a primary proton beam with a kinetic energy of 8 GeV and a power equal to 8kW, but how?

Two Booster proton batches are extracted into the MI-8 beamline and injected into the Recycler Ring. There the beam circulates for 90ms while a 2.5MHz bunch formation RF sequence is performed in order to obtain from each bunch four 2.5MHz bunches that occupy one seventh of the circumference of the Recycle Ring.

Each of these bunches is synchronously transferred, one at-a-time through existing transfer lines, to the Delivery Ring. Then the beam is held in a 2.4MHz RF bucket during resonant extraction to the experiment through a new external beamline. To control the spill rate uniformity during resonant extraction a technique known as RF

¹CLFV: transition among μ e τ that doesn't conserve lepton family number[3].

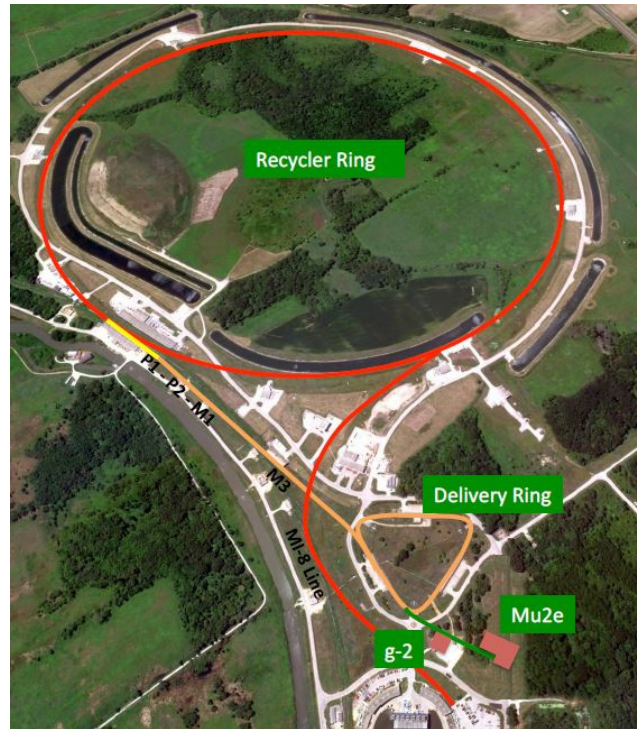
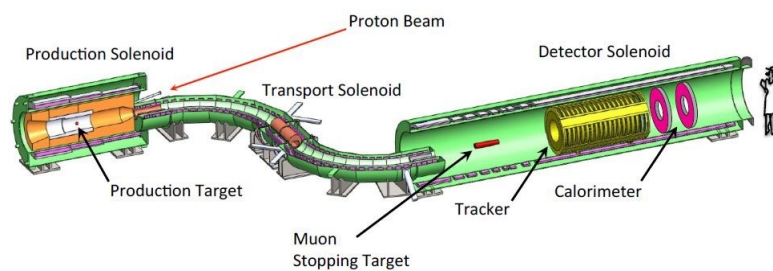


FIGURE 1.1: Layout of the Mu2e facility (Accelerator complex that provides proton beam to the detector.).

knockout will be used. The resonant extraction system will inject 3×10^7 protons into the external beamline every $1.7 \mu\text{s}$, an extinction system is required to suppress unwanted beam between successive pulses.

The proton pulses not suppressed are delivered to the production target located in the evacuated warm bore of a high-field superconducting solenoid. The proton beam obtained will have a transverse radius of 1mm and a duration of 250ns.



from "TDR Final" October 2014

FIGURE 1.2: The Mu2e Detector (The cosmic ray veto that surrounds the Detector Solenoid is not shown.).

The production target (PT) is a radiatively cooled tungsten rod with the size of a pencil, downstream this target an air-cooled beam absorber is used for unspent beam. All these elements are contained in the production solenoid (PS) which is a high field magnet with a graded solenoidal field varying smoothly from 4.6T to 2.5T, it is approximately 4m long and its bore diameter dimension is 1.5m. This volume is

evacuated to 10^{-5} Torr, and a lining shield against heat and radiation is used to protect solenoid's superconductive coils. The aim of the PS is to capture pions and the muons into which they decay, guiding them downstream to the transport solenoid (TS).

The TS S-shaped solenoid efficiently transmits low energy negatively charged muons to the detector solenoid (DS), the rest is eliminated by absorbers and collimators.

The DS is a large low field magnet in which there's the muon stopping target (MST) and all the components related to the analysis and detector phases. It's 11m long and the bore diameter is about 2m, the magnetic field varies from 2T to 1T and it captures the conversion electrons emitted in the opposite direction of the detectors but has also a role into reducing the backgrounds.

The detector components are placed in a volume evacuated to 10^{-4} Torr with a relatively uniform magnetic field. The detector is designed to efficiently and accurately identify and analyze the helical trajectories of electrons with an energy of 104.97MeV. It mainly consists of a Tracker and a Calorimeter that provide redundant energy/momentum, timing and trajectory measurements. The tracker measure the trajectory of the electrons in a uniform 1T in order to determine their momentum.

Chapter 2

Mu2e Tracker

The Mu2e tracker is the most important part between the detector elements. It must provide a good resolution based on background rejection that mainly consists in Decay-In-Orbit (DIO) electrons¹ with the normal Michel endpoint at $52.8\text{MeV}/c$ [2]. In presence of a nucleus the outgoing electron can exchange a photon with the nucleus itself reaching an energy of $105\text{MeV}/c$ (equal to that of a conversion electron ones).

2.1 Straw



FIGURE 2.1: Straw (Metalized Straw tube, [7]).

The Tracker is made from 5mm diameter straws (Figure 2.1). Each straw is made of two layers of $6.25\mu\text{m}$ Mylar, spiral wound, with a $3\mu\text{m}$ layer of adhesive in between, for a total thickness of $15\mu\text{m}$. The inner surface has 200\AA gold over 500\AA aluminum to serve as cathode. The outer surface has 500\AA of aluminum for additional electrostatic shielding and to improve the leak rate. The drift gas is 80:20 *Argon* – *CO*₂.

A gold-plated tungsten sense wire of $25\mu\text{m}$, that is the basic detector element, is placed during the assembly inside the tube thanks to an injection molded plastic with an epoxied brass U-shaped pin in which the wire is soldered. The molded plastic with the U-pin are connected to the straw with a brass tube

The detector has 20040 straws in total distributed into 20 measurement stations across 3m length. Each straw is instrumented on both sides.

2.2 Panel, Plane, Station

Group of 96 straws are assembled into panels, as shown in Figure 2.2. Each panel covers an arc of 120° with two staggered layer of straws (solving the problem of the

¹DIO: The process is $\mu^- \rightarrow e^- \nu_e^- \nu_\mu$.

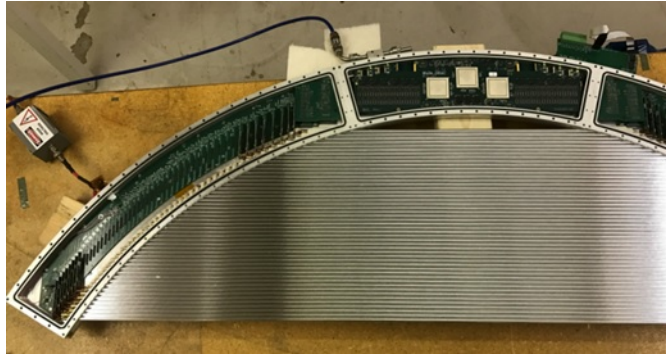


FIGURE 2.2: Instrumented Panel [7].

so called "left-right" ambiguity). The intent is to cover the radial range from 380mm to 680mm as uniformly as possible and keeping electronics outside the active region. The structure is completed by an inner ring, a base plate, an outer ring, a cover and screw and O-rings. The straws are aligned with the Panel Assembly and Alignment System (PAAS) separately from the wires to avoid cumulation of errors. Each panel requires the following utilities:

- Gas lines (supply and return) made with stainless steel tube epoxied into a hole in the outer ring;
- Standard power (supply and return) for vacuum feedthroughs;
- High voltage single line;
- Copper signal lines;
- Optical signal lines.

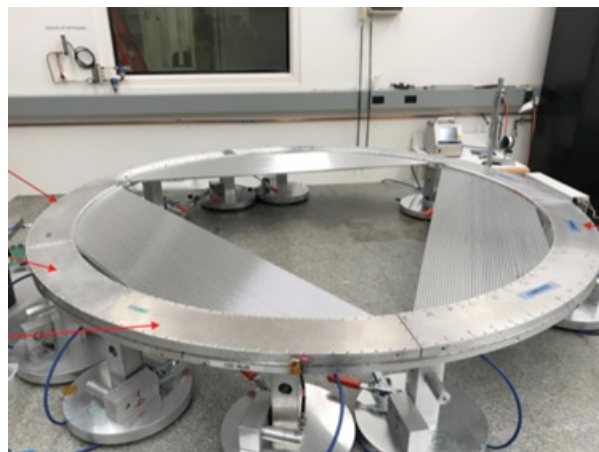


FIGURE 2.3: Half Plane on granite assembly table [7].

Six panels are assembled into a plane (Figure 2.3). Three 120° panels complete the ring of one face, then another three panels rotated by 30° completed another ring on the opposite face. After the assembly of the plane, a cooling ring is attached around the outer diameter. A pair of identical planes, the second one rotated around the vertical axis of 180° forms a station (Figure 2.4).

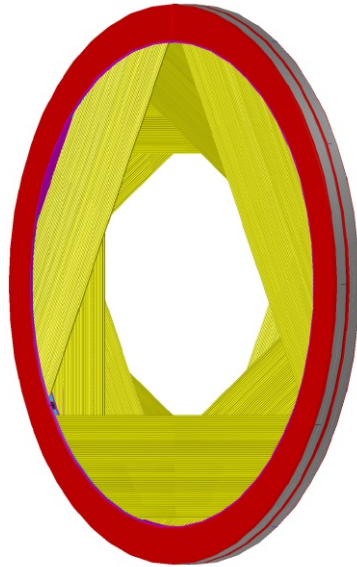


FIGURE 2.4: Station

2.3 Frame

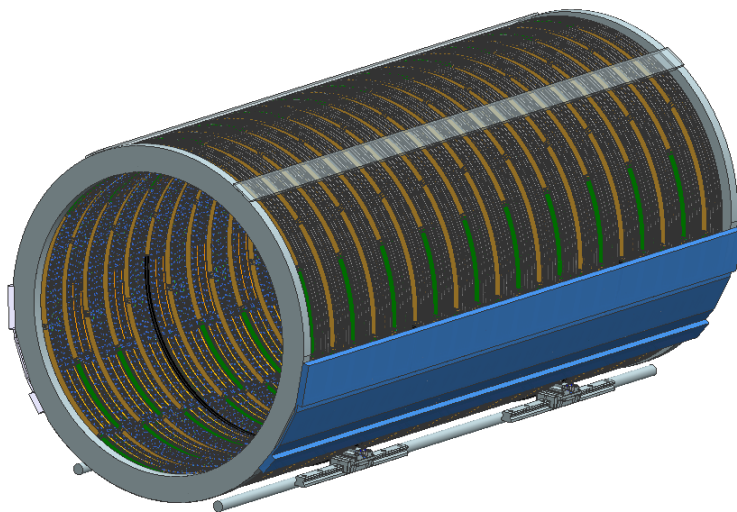


FIGURE 2.5: Tracker (the straws are not shown).

The complete tracker is made up of 20 stations which are held together by a structure called "frame". The so called structure has two wide horizontal beams (called staves) near 0° and 180° that carry power, signal and gas lines. A third beam at 270° is used to maintain spacing, all these beams are outside the active volume. Two support rings near the front and the back are provided to increase the stiffness of the structure, some other else along the length are used as shielding. Including the support structure the tracker has a radius of 850mm and a length of 3270mm.

Chapter 3

Problem Definition and Design Requirements

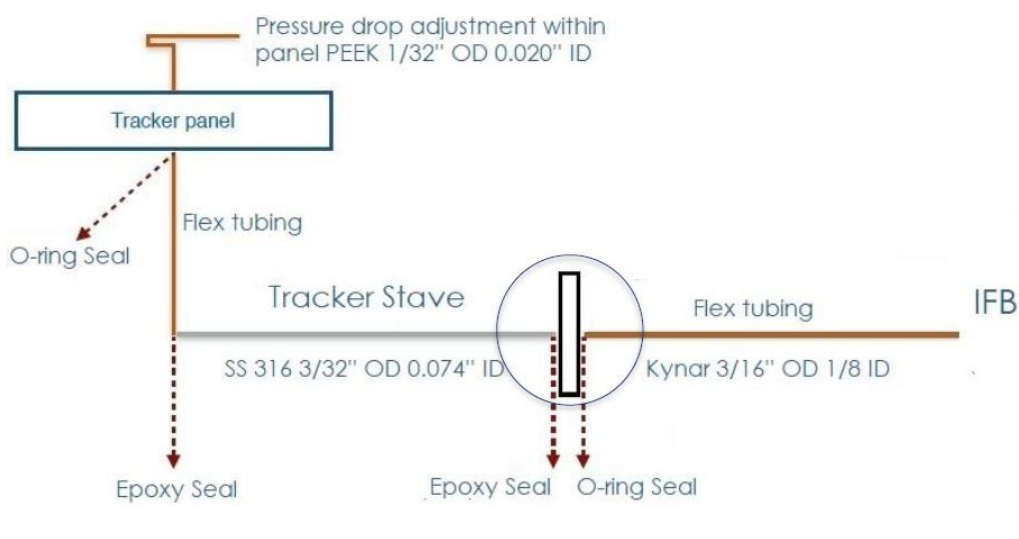


FIGURE 3.1: Line (A preliminary Scheme, [10]).

We have already said in Section 2.1 that the basic detector element are the straws which work with a gas mix. This *Argon* – *CO₂* mix enters (and exits) in the DS volume through the IFB using 216 kynar^{®1} tubes and must feed all the panels that are equipped with different stainless steel (SS) tubes (Figure 3.1, the blue circle underlines the connection).

The main object of my activity was focused on how to connect these two groups of tubes.

3.1 Problem Definition

Although some things were already explained, some additional considerations are required to understand the starting point, in particular some questions that can arise could be:

- Why we need 216 standalone lines? it's worth to notice that this is equal to the number of the panels², the necessity to feed each panel separately improve the general reliability. For example in case of failure of a straw we can be able

¹Kynar[®] is a plastic material already tested for outgassing and resistance to radiations, more information can be found in Mu2e Docdb 27691-v1.

²We have in total: 18 stations, 2 planes for each station, 6 panels for each plane.

to stop the feeding on the specific panel experiencing the minimum lose on the detecting power, we must also underline that the Tracker is designed to operate without repairing operations with a 90% confidence for a year;

- Why the tubes are not equal? On the Tracker side the volume available is a third of the volume on the Calorimeter side³, this led to choice metallic tubes. This configuration has as result to keep the internal diameter of the tubes approximately the same so the pressure drop isn't affected but the wall thickness is smaller saving space as needed.

After this general overview let's define the quantitative constraints.

3.1.1 Geometric Constraints

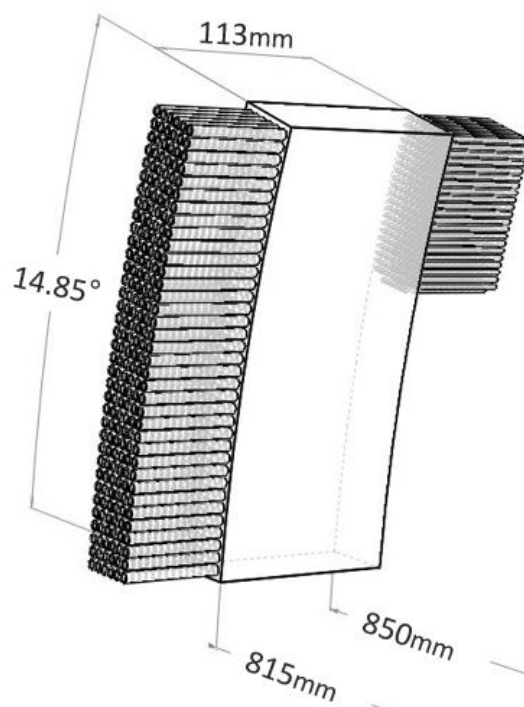


FIGURE 3.2: Volume available with tubes (On the left the Calorimeter or IFB side and on the opposite the Tracker side).

The available volume is an arc of an holed cylinder whose:

- Axial dimension is equal to 113mm;
- The inner radius is equal to 815mm;
- The outer radius is equal to 850mm;
- The angular span is equal to 14.85° on the Calorimeter side and only a third on the Tracker side (5.0257°);
- The outer diameter of the kynar tubes is equal to 4.76mm;
- The outer diameter of the SS tubes is equal to 2.38mm;
- The minimum radius for a channel is 0.93mm;

³The remaining area is occupied by the "Key" for more information about this aspect refers to [10].

3.1.2 Working Constraints

Some other constraints are connected with the working conditions required as:

- The flow in the straws must provide a volume exchange for the manifolds and the straws per hour (that is equal to two straws volume exchange per hour) then the flow rate is $\Phi = 9.6 \times 10^{-7} \frac{m^3}{s}$;
- The internal pressure in the straws is the atmospheric ones (15psi) so the pressure into the lines must cover the losses that are preliminary estimated as 0.04psi (taking in account only distributed losses [11]);
- The external pressure is the DS pressure (10^{-4} Torr);
- The seals must not affect the vacuum pressure level over the general limit, the total common budget of the project for the outgassing rate is equal to 3sccm⁴;
- The materials used must not affect the magnetic field, also for this reason aluminum or low carbon steel are widely used;
- The materials used must resist to the environment radiation level.

⁴sccm stands for Standard Cubic Centimeter per Minute

Chapter 4

Preliminary Design and Analyses

4.1 Preliminary Design and General Considerations

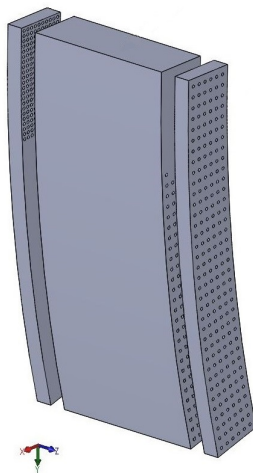


FIGURE 4.1: Preliminary General Design (Incomplete).

The idea behind the general design was conceived in the first middle of the program and although several updates it remained almost the same. Figure 4.1 shows the first model developed made up of a printed part positioned in the middle with two interfaces on the extremities.

4.1.1 Printed Part

The solution just showed was chosen after a comparison with some other possibilities, a short overview can clarify what were the other ones evaluated and the why we chose this particular way.

The other possible scenarios that we take in account were basically two:

- To bend the tubes avoiding the interfaces and the printed part. The issues related to this solution was surely that would have been more expensive but also the condition on the minimum bending radius that must be at approximately 5 times the outer diameter would have been a great problem;
- To use welded or epoxied elbows. This can be considered a solution to the problem of the space but remain the high cost connected with the welding (or epoxying) process.

After stating that adopting a solution based on a printed part was our best chance there were always few degrees of freedom on how to design it, in particular the following decision that I took was to use a spline curves-based pattern for the channels instead of a linear-based pattern. Starting from the idea to use a printed part we gained, for itself nature, wide geometrical possibilities in which I saw possible advantages as:

- Smooth paths reduce the losses;
- Regular channels avoid all the phenomena connected with sharp change of the flow;
- Take care of the geometry can simplify the printing phase but not only, if the polymerized leves are stacked along z-axis¹ the structure would be self-supporting and this would led to best results in terms of resolution and precision.

4.1.2 Connectors

It's worth to notice that tubes could be linked with the model using epoxy but having something as a connection that can be removed or installed in situ enormously simplify the assembly (and unexpected replacements).

I used a considerable amount of my time on the connectors because the service elements are obviously routed taking in account the needs of all the groups involved, in this scenario "smart" connections can avoid danger operations that aren't in the specific responsibility of a single group. For all these reasons all the following models will include also the so called "connectors". They are placed only on the calorimeter side, for two basic reasons:

- Using them on both sides won't carry more advantages then on one side only. The SS tubes are included in the Tracker design and can be routed and connected to the model in the laboratory before going to the installation site;
- There isn't enough space on the Tracker side.

4.1.3 Interfaces

The interfaces showed in Figure 4.1 reflects the first concept in which we adopted them to manage the connection with the tubes.

We knew that the extremities should have been quite different from the printed part itself. Since that they strongly depends on connectors, this aspect necessarily came after the progress made with them.

4.1.4 Blocking System

Although the use of connectors take some advantages there're some issues that must be taken in account, in particular the technical solution must prevent the accidental pull-out by the pressure². For this reason a general design of a blocking system must be included respecting all the constraints listed.

¹The z-axis specified is based on the Mu2e CS, for more information refers to Mu2e docdb 1383-v7.

²The differential pressure during normal working conditions pushes the connector out.

4.2 Preliminary Analyses

The preliminary analyses regarded the achievable clearances in order to confirm the feasibility and machinability of a printed part.

As said in Sub-Section 3.1.1 and showed in Figure 4.2 the available angular dimension change along the z-axis then some changes of pattern must be done to use rationally the current surface. The simplest way to place the holes is a regular pattern along radial and circular direction, with it we can reach a minimum clearance of³:

- On Calorimeter-Side: 3.38mm;
- On Tracker-Side: 1.31mm.

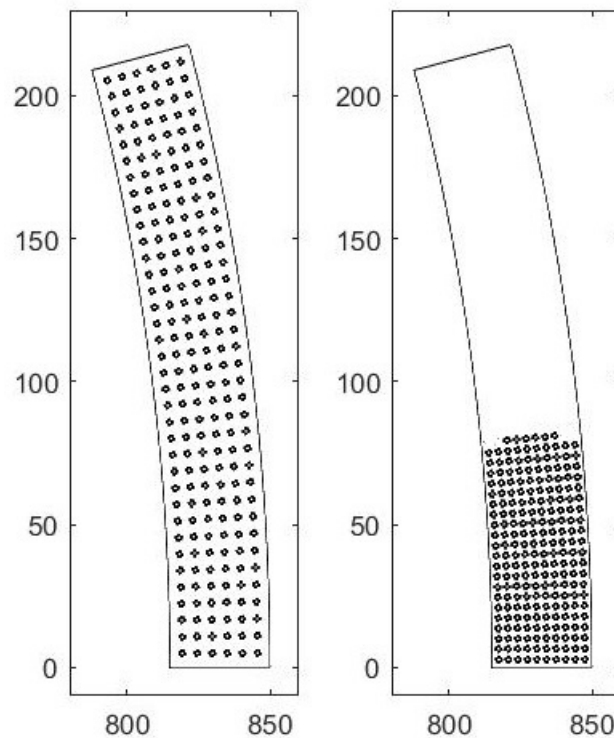


FIGURE 4.2: Regular Pattern (Calorimeter Side on the left:36x6 - Tracker Side on the right:22x10).

As consequence of these considerations the minimum expected thickness is 1.3mm. Before going on with the modelling phase (although the loads are really low) we decided to perform a rough stress analysis. Some load cases (LC) are been considered as:

- LC of channel connected with a panel that leaks ($p_{in} = 0psi, p_{out} = 16psi^4$);
- LC of normal working conditions ($p_{in} = 16psi, p_{out} = 16psi$);

³We are considering holes with the radius equal to 0.9398mm as specified in Sub-Section 3.1.1

⁴This pressure must be intended as an overestimation of the normal working pressure as far as there isn't a better data to use.

- LC of maintenance operation ($p_{in} = 16\text{psi}$ ⁵, $p_{out} = 19\text{psi}$ ⁶).

The assumptions used to built the model are listed below:

- The simulation models static conditions (stationary case);
- The connection between the printed part and the interface on the stave side is modelled as "fixed support", the study of the local solution go over the intent of this preliminary analysis, end effects must be ignored;
- The connection between the printed part and the interface on the IFB side is modelled as "free surface", under the hypothesis that the actions of the flexible tubes (kynar[®]) are negligible and that the internal actions of the epoxy will produce only local effects ignored as above;
- The gravity effects are ignored, the printed part is in UV cured epoxy so its weight is negligible, we don't know also how the tubes are supported precisely, so we cannot estimate the gravity loads that come from them;
- The only load applied is the inside and outside pressure depending on the LC, to be conservative the outside pressure is constant and equal to the maximum value;
- The geometry is simplified using a conservative approach, a tube of the minimum thickness represent the single channel;
- The material is modelled as elastic isotropic, more mechanical properties are needed to go further;
- The mesh used is mapped and the size is 4 times less than the diameter of the tube.

The worst LC is the first one, a scheme and the Von Mises equivalent stress is presented below in Figure 4.3. Since the maximum stress level registered was about

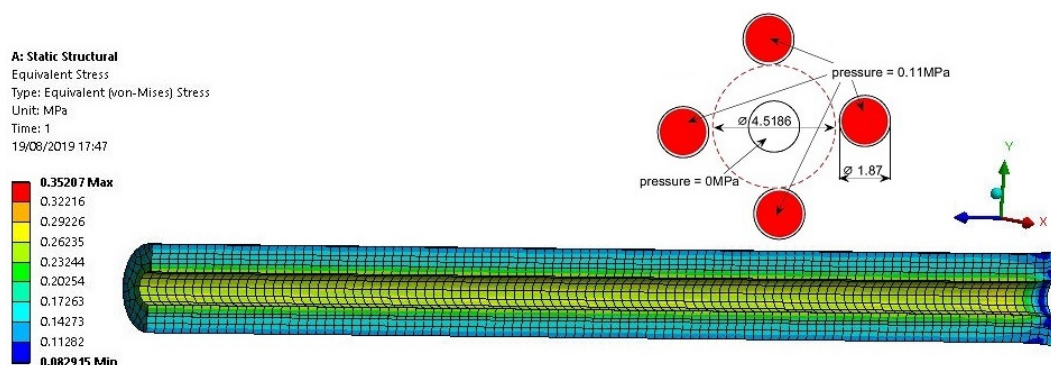


FIGURE 4.3: Worst LC scheme and Von Mises equivalent Stress.

0.28MPa using a printed part is a possible way⁷, the mechanical analysis can be refined and repeated with the final design.

⁵It's fundamental to ensure this pressure in order to prevent the collapse of the straws under the external pressure.

⁶During the maintenance operations the DS must be back-filled, this value is the pressure level required to have access to the magnet.

⁷Common UV cured epoxy already used has a tensile strength above 50MPa, Somos[®] PerFORM can be a good candidate.

Chapter 5

Printed Part

The following chapter is divided in two main parts to underline the design process that in the same way was carried out in two steps.

It's important to enlight that the final approach, that can appear as much more than the necessary, was used only because a light one failed on meeting the requirements. Since that in Sub-Section 4.1.1 we decided to use a printed part with a spline curves-based pattern, we can list some additional requirements that must be met:

- In Section 4.2 was reported that the minimum clearance is reached on the Tracker-side where the available angle-arc is the minimum one. The idea is to preserve this clearance and to not go down;
- It's important to have a regular channels and to avoid ripples where isn't strictly necessary;
- Straight ends must be provided in order to avoid abrupt change from the interfaces to the printed part.

In order to save time in a process that appeared to be subjected to continuous refinements, I decided to use MATLAB[®] to have a flexible geometry that could be easily updated.

The idea is to use a script which aims to write a database of points that can be used for the channels' centerlines then to read it with a Macro in the CAD environment drawing automatically the just mentioned lines.

As help on the debugging phase the script provides also a graphic result.

5.1 First-phase approach

As said in Section 4.2 a rational use of the available volume requires a change of pattern. I already showed that on the tracker side the best one is a 10x22¹ and that on the calorimeter side is a 6x36. Since that the angle-arc change in intended as a monotonic function we can expect that there're inner planes in which switch to intermediate configurations (as 9x24, 8x27 and 7x31) would increase the clearance. Someone can observe that it worth nothing increase the clearance somewhere if the minimum one is still the same, this is obviously true but reducing the volume that represent the weakest condition it's costless and could low the risks connected with unpredictable defects of the material.

¹This way to describe the pattern must be intended as (holes on radial direction)x(holes on circular direction).

5.1.1 Script description

As long as the complete script can be request if necessary², here I want to do only a short overview on how it works:

- The constants and the parameters are defined (as geometric dimensions and other useful informations);
- The z-coordinates where the switching to another pattern is recommended are found checking the clearance using the current configuration or the following;
- If the pattern is changing on the current z coordinate all the points that built the pattern are recorded in a file called "My_file". At the end it contains 1085 points;
- A cell structure called "Matrix" is initialized, it contains a number of matrices equal to the number of planes and each matrix has the dimensions of the pattern all the elements are setted to "1" (that means that that point isn't used);
- A cell structure called "curves_database" is initialized, it contains a number of matrices equal to the number of the channels (216);
- A "Ruler" decided how to match the points on the planes³. The simplest rule that I found works as "check in the matrix that rapresent the next plane , who is the first available element?, if it's one column on the right use it; if don't must be on your same column, take it", set it equal to the number of the curve (that means that the point is used) read its coordinates in "My_file" and record them in the element that rapresent the current channel in "curves_database".

5.1.2 First-phase results

The final result is that the elements of "curves_database" contains 5 points one on each plane and the elements of Matrix are named as the curve's number that passes through that position⁴. Using the structures just above I was able to draw auto-

curves_database{13, 1}			
	1	2	3
1 5x3 double	1 819.1638	16.4383	93
2 5x3 double	2 818.5340	14.9240	63.2400
3 5x3 double	3 818.0550	12.9670	37.2000
4 5x3 double	4 817.6680	11.4290	19.5300
5 5x3 double	5 817.3520	9.9380	0
6 5x3 double	6		
7 5x3 double	7		

Matrix{3, 1}		
	1	2
1 36x6 double	1 1990	2050
2 31x7 double	2 1930	1940
3 27x8 double	3 1870	1880
4 24x9 double	4 1810	1820
5 22x10 double	5 1750	1760
6	6 1690	1700
7	7 1510	1570

FIGURE 5.1: Cell Structures: "curves_database" on the left, "Matrix" on the right.

matically all the curves on SolidWorks[®] (and on MATLAB[®] as shown in Figure 5.2)

²The script length is 900 lines and requires 2 additional functions, it can't be listed in the appendices.

³The elements are runned from the left to the right, from the low to the top, because in the same way the points are stored in "Myfile".

⁴The elements of Matrix are multiplied by 10 to avoid some issues, as shown in Figure 5.1.

but the problem was that between each couple of planes, during the transitions, the curves became closer and the clearance went often down until 0.3mm.

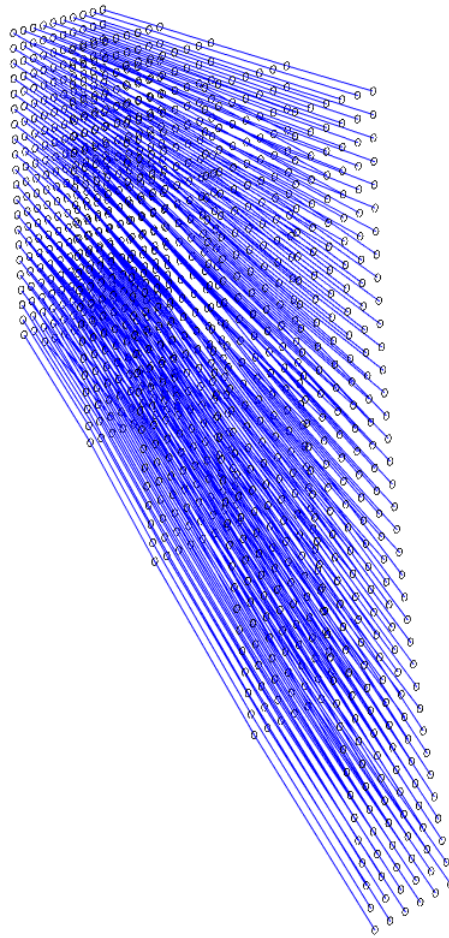


FIGURE 5.2: MATLAB® First-Phase Result.

5.2 Second-phase approach

All the experience achieved clarified that a deep control was absolutely needed. The first part of the script appeared to be an excellent starting point to be updated since that the problems weren't conceptual errors in it but related to a too weak control. The first attempt was to reinforce the control using more planes, recording also the z-coordinates where the pattern doesn't change but it failed, then a more accurate and radical change was made.

5.2.1 Script description

This second part of the script is just added to the first one, the basic idea is to enrich the previous "curves_database" with new points.

Before going on with the overview it's worth to enlight that this part consequentially works on the transitions between the previous five planes⁵ with a step equal to 1mm.

⁵For example at first all the z-coordinates between Matrix(1,1) and Matrix(2,1) are runned, then all the z-coordinates between Matrix(2,1) and Matrix(3,1) and so on.

In each z-coordinate all the curves are update before continue to next new plane.

- The curves are retrieved from "curves_database";
- Knowing their number, all the curves near the current one in the starting and ending transition planes are recorded as "neighbors"⁶;
- Using a spline a first aestimation of the point on the current z coordinate is found;
- Some checks point out if the aestimation respects the minimum distance from the external surface, if it doesn't it moves slowly in;
- Some checks point out if the aestimation respects the minimum distances from the neighbors already updated in the current z coordinate, if it doesn't it moves slowly far from the nearer and towards the farer curves;
- Some final checks point out if the aestimation respects the minimum distance from the external surface, if it doesn't it moves respecting the distances from the neighbours;
- If all the conditions are met the new point is stored in "curves_database" and it results as "updated" in the current z coordinate.

5.2.2 Second-phase results

The maximum global clearance that could be reached is 1.3mm, the script reached a value between 1.25mm and 1.28mm. An overview of the MATLAB graphic output during a run can be found at [MATLAB A. Fino Script](#)⁷.

I used the old macro with the new database to built the new 3D model, then to double-check the result I performed also a thickness analysis (Figure 5.4).

Thickness Range	Total Surface	Surface Percentage
From 1.2mm to 0.9mm	269.63mm ²	0.13%
From 0.9mm to 0.6mm	12.42mm ²	0.01%
From 0.6mm to 0.3mm	1.25mm ²	0.00%
From 0.3mm to 0mm	0.38mm ²	0.00%

Excluding some small spots on the extremities that are wrongly read by the tool all the thickness is more than 1.2mm.

It's worth to notice that saving more space on the external part I was able to cut that material and to use that space for the blocking system.

⁶Take a look on the right side of Figure 5.1, the curves that are around aren't obvious since that they has an order on the first plane but after that they start to change pattern.

⁷The red circles showed have a radius that is the r_{hole} plus half clearance ($\frac{1,3}{2}$)mm.

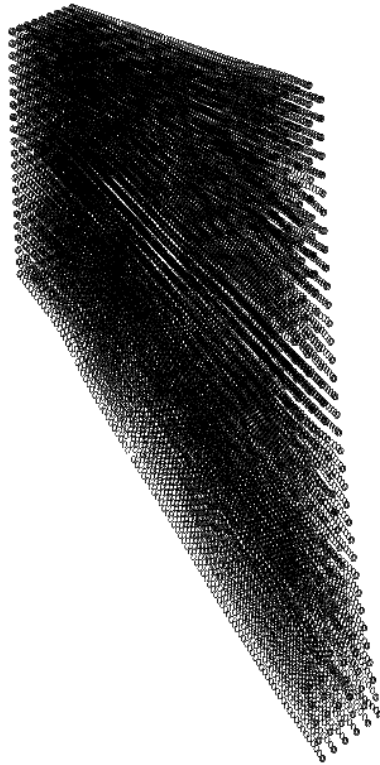


FIGURE 5.3: MATLAB[®] Second-Phase Result.

5.3 Conclusion

The solution met all the requirements, the transition is quite smooth, the clearance is good and all the constraints are respected.

We asked for a cost-estimation to some Fermilab's external suppliers and the amount is around 1000-1500\$ for each part⁸.

⁸We need two of them, one for the inlet and one for the outlet.

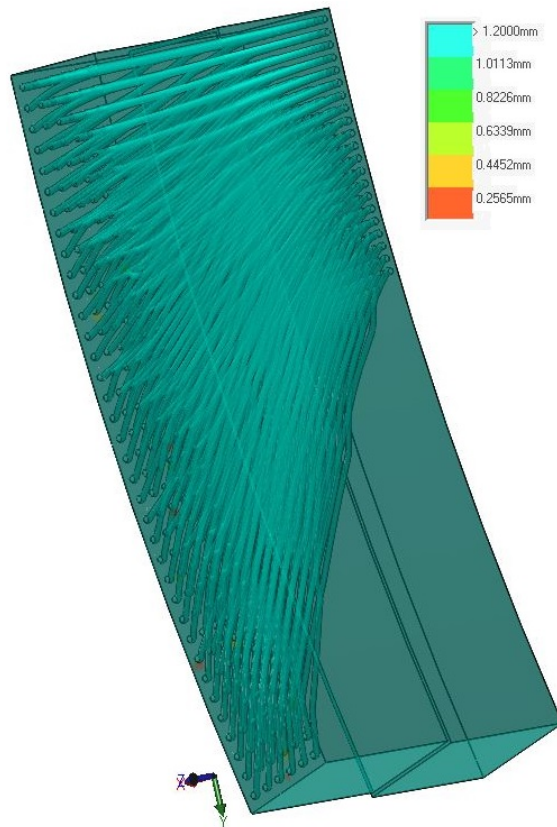


FIGURE 5.4: SolidWorks Thickness Analysis.

Chapter 6

Connectors

Figure 6.1 represents circles with the outer diameter equal to the kynar[®] tubes' ones¹, the clearance between them is about 0.5mm.

This two lines stated that the we have a circle with a diameter of 5.26mm in which we must include:

- The connector itself;
- The clearance.

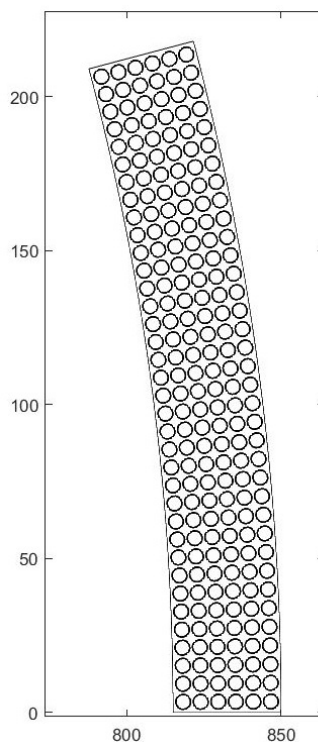


FIGURE 6.1: Calorimeter Side with Kynar[®] Tubes:clearance available.

6.1 Preliminary design ideas

Starting from as simple as possible ideas some research on sealing connector solutions are carried out. The first solution (Figure 6.2) uses a radial sealing and a

¹The outer diameter of kynar[®] tubes is approximately 4.76mm.

bushing. A small insert epoxied in the kynar[®] tube has a groove for an O-ring that guarantees the seal using a bushing² epoxied in the printed part.

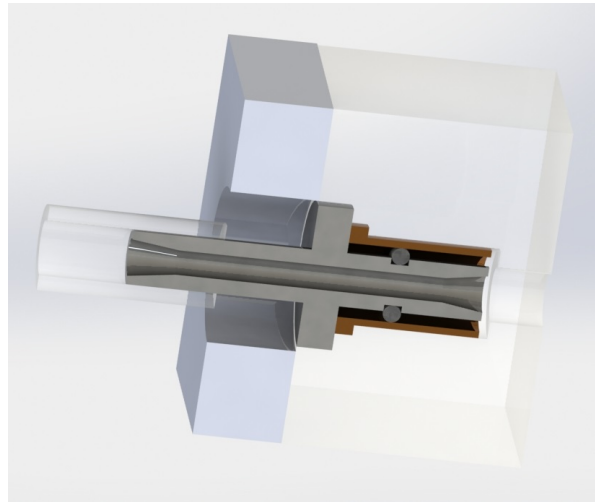


FIGURE 6.2: Connector: Radial Seal with Bushing.

The advantages are that it is simple, some parts can be found off the shelf and that this kind of sealing has been already tested and met the requirements.

The main disadvantage is that in this case we must provide something that can prevent the pull-out of the connector.

The second solution (Figure 6.3) uses a tapered sealing and a threaded connection. The insert is still epoxied in the kynar[®] tube, it has two opposite tapered surfaces, the threaded connection provides the load that holds the insert pushed towards its seat making the seal.

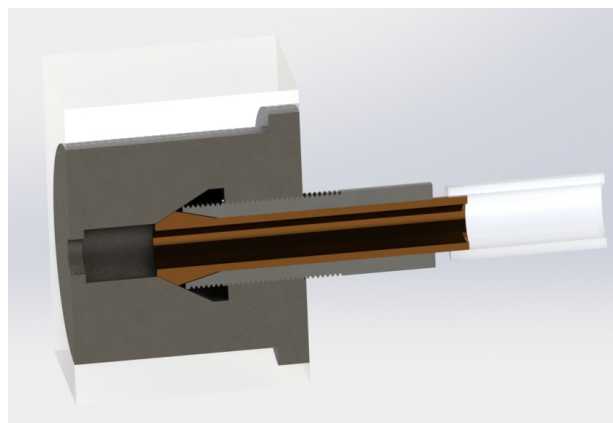


FIGURE 6.3: Connector: Tapered Sealing with Threaded Connection.

The advantages in this case are that this solution is widely used in high pressure valves so it can work also in our case and that the threaded connection prevents the pull-out, no additional elements are required.

The disadvantages are that more space is required, complex machine operations and high precision must be guaranteed and that the solution is entirely custom, nothing

²The bushing is used to provide a surface with the required finishing.

can be found off the shelf.

The last solution (Figure 6.4) uses an axial sealing and a threaded connection. The insert is always epoxied in the kynar[®] tube, the threaded connection provide the load that pushes the O-ring between the two planar surfaces making the seal.

This design is quite simple, can fit and the threaded connection prevent the pull-out, but more space is required.

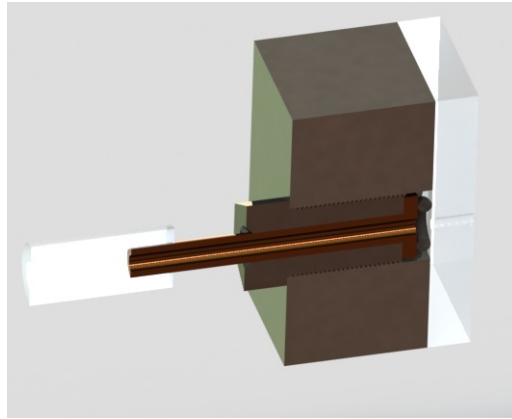


FIGURE 6.4: Connector: Axial Sealing with Threaded Connection.

6.2 Actual Design

Since that the dimensions are the main issue we judged the first solution (Figure 6.2) the best candidate, in the following sections all the steps required to reach the final design (Figure 6.5³) and then to test it are reported.

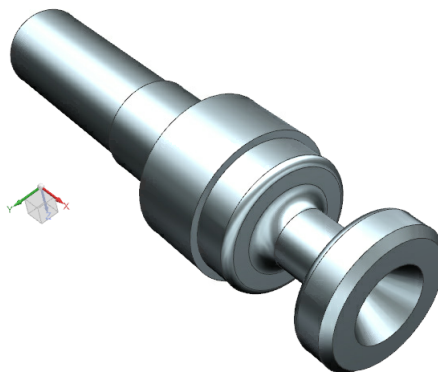


FIGURE 6.5: Connector: 3D Model on NX[®].

6.3 O-ring Study

One of the key elements of this model is the O-ring (OR). An OR must be deformed to act properly, if it isn't squeezed and stretched in its application it isn't the correct one.

³Part no. on TeamCenter[®] F10127000 (3D and 2D), Author: Andrea Fino.

The three most relevant characteristics for an OR are its inside hole diameter (ID), its cross section (CS) and the durometer that measures the hardness of an elastomeric compound⁴.

In general a seal can be activated by two mechanisms, the OR can be forced thanks to:

- The geometry itself that is set up to realize the correct amount of deformation;
- The high pressure that pushes the OR on the low pressure side.

In our case we don't have high pressure⁵ so the only possibility is to take care of the geometry and to rely solely on the resiliency of the elastomer to retain its original compressive force⁶. In order to obtain the deformation required two recommendations must be satisfied:

- The ID must be smaller than the piston groove diameter, the stretch should be between 1-5% with an ideal value of 2%. A stretch greater than 5% is not recommended because it can accelerate the aging process and because it reduces the CS. We want to use an off the shelf OR so this condition will be on the insert groove diameter;
- The gland depth⁷ (or the bore diameter) with the CS directly influences the amount of compression that must be between 10-40%.

The deformation itself isn't enough, another fundamental factor is the surface finishing. For static glands an RMS from 64 to 128 micro-inches can be tolerated, however a finish of 16 micro-inches is recommended for gases and vacuum applications.

In any sealing application, the tolerances of all the parts in contact with the OR must be considered in order to create the effective seal. The combination of these tolerances is the tolerance stack-up, if the OR is very small (as in our application) the tolerances are larger (in relative terms) and manage them isn't simple.

In pneumatic or vacuum applications, where fluid are predominantly absent, OR surface lubrication is mandatory⁸, it prevents leakage by filling micropores of both the O-ring and surrounding metal surfaces.

In vacuum application where the low gas permeability and the low weight loss are fundamental one of the best compounds is the Viton⁹. We have two different choices on the OR choice, the first is to take a standard off the shelf one, the second is to take a non-standard off the shelf one.

6.3.1 Standard Off the Shelf

The only Standard¹⁰ OR that can fit with our application is the 004 (Figure 6.6), the 003 is too small and the 005 is too big.

The Standard OR has several advantages like:

⁴The numerical ratings for hardness run from lower numbered (less than 70) softer materials to higher numbered (greater than 70) hardened materials, noting that fluorocarbon has a base of 75.

⁵If the system pressure is lower than 100psi is judged as a low pressure application.

⁶Over the time, the elastomer will not resist compression as much as take a compression set, resulting in possible seal failure.

⁷The gland depth is the sum of groove width and half diametrical clearance.

⁸Make sure to use a lubricant that is compatible with the OR's compound and the chemical substances used.

⁹Viton is a fluoro-elastomer widely used for OR.

¹⁰The Standard is the AS-568.

AS-568 NO.	NOMINAL REFERENCE			ACTUAL DIMENSIONS	
	I.D.	O.D.	Width	I.D. Tol.	W. Tol.
-004	5/64	13/64	1/16	.070 ±.005	.070 ±.003

FIGURE 6.6: OR 004 AS-568: Geometry.

- All sellers have it, so it's simple to find it from the seller that you prefer and from who the materials have already been tested;
- The seal geometry is suggested by the standard.

The standard solution has also some disadvantages like:

- A smaller hole in the insert that lead to an increase of the pressure drop or/and to a decrease of the wall thickness of the insert;
- A bigger hole for the gland (not enough space for the bushing).

6.3.2 Non Standard Off the Shelf

¹¹ The non-Standard Off the Shelf OR has one relevant advantage, it has less geometric constraints that allow to use a smaller hole for the gland and to reach a higher wall thickness for the insert.

In Figure 6.7 the red crosses are some available ORs from a specific vendor, the horizontal axis represent the ID, the vertical axis represent the CS.

This graphic help in the selection of the OR, in particular:

- The ID of the insert is calculated from the ID of the OR using the condition on the stretch;
- The two lines are drawn starting from the assumption that the bore diameter is equal to 4.26mm¹². The knowledge of the ID (as stated in the previous point) and the bore diameter using the condition on the compression (minimum and maximum value) gives the minimum and maximum CS that can be used.

In the red circle there're the best ones that allow to have the greatest IDs¹³.

The non-Standard solution has surely disadvantages too, they are specific from a vendor and a custom gland geometry must be setted up and tested.

6.3.3 A Brief Comparison

Although the Non-Standard OR ensure a better geometry (Table 6.1), the chance to use a material already tested from a well-known supplier it's more relevant, for this reason we decide to use the 004.

¹¹For the formulas please refer to Appendix A.

¹²This ensure to have a clearance equal to 1mm.

¹³As already said for the Standard OR a greater ID can be used to high the wall thickness of the insert or/and to have a greater inner hole to low the pressure drop.

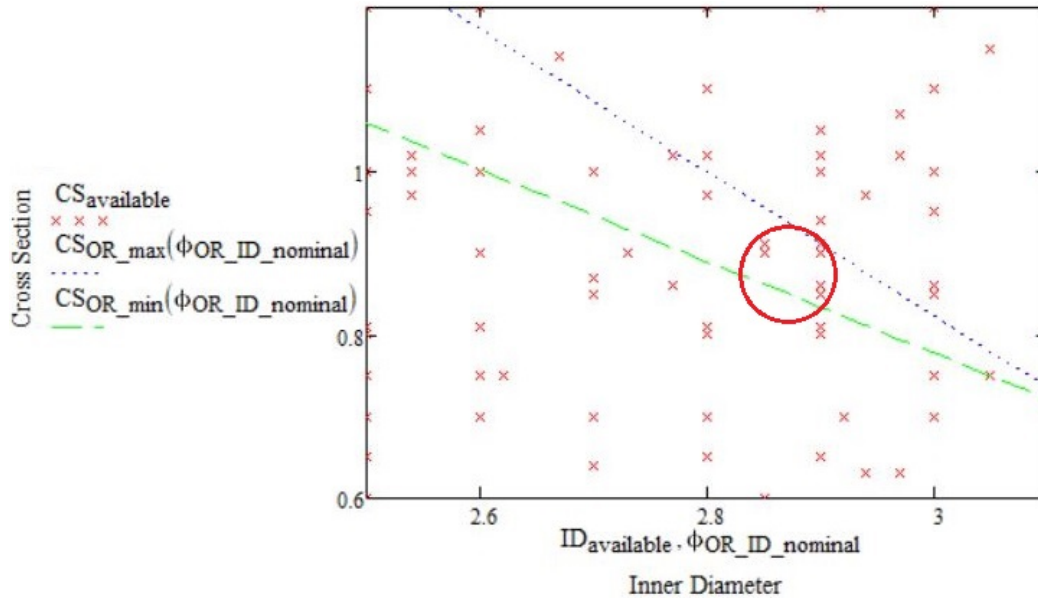


FIGURE 6.7: Standard ORs (range of CS and ID that could fit with the application).

	Bore Diameter	Piston Diameter
Standard Solution 004	0.181in	0.08in
Non Standard Solution	0.167in	0.112in

TABLE 6.1: Standard and Non Standard OR Solutions.

6.4 Pressure Drop Evaluation

The next step is to evaluate the pressure drop related to the connector.

With the hand calculation¹⁴ I found an overestimation of the losses, the transition were modelled as abrupt changes, the result is $\Delta p_{tot} = 6 * 10^{-4} psi$.

I also performed a basic CFD analysis on FLUENT^{®15} (Figure 6.8), this way led to an underestimation because I used the hypothesis of laminar flow, the result is $\Delta p_{tot} = 2 * 10^{-4} psi$.

Considering a nominal value of 0.05psi¹⁶ the drop is negligible because less than 1.1%.

6.5 Equipments

A simple equipment was necessary to test and to measure the leak-rate. The main aspects that influenced the design of the apparatus were the minimum time available and to prefer simple design choices in order to have parts that can be machined in the Fermilab's Machine Shop.

¹⁴For the formulas please refer to Appendix B.

¹⁵This model doesn't have too much details to explain, I used the inner surface of the insert and the correct speed at the inlet.

¹⁶For more details please refer to Sub-Section 3.1.2

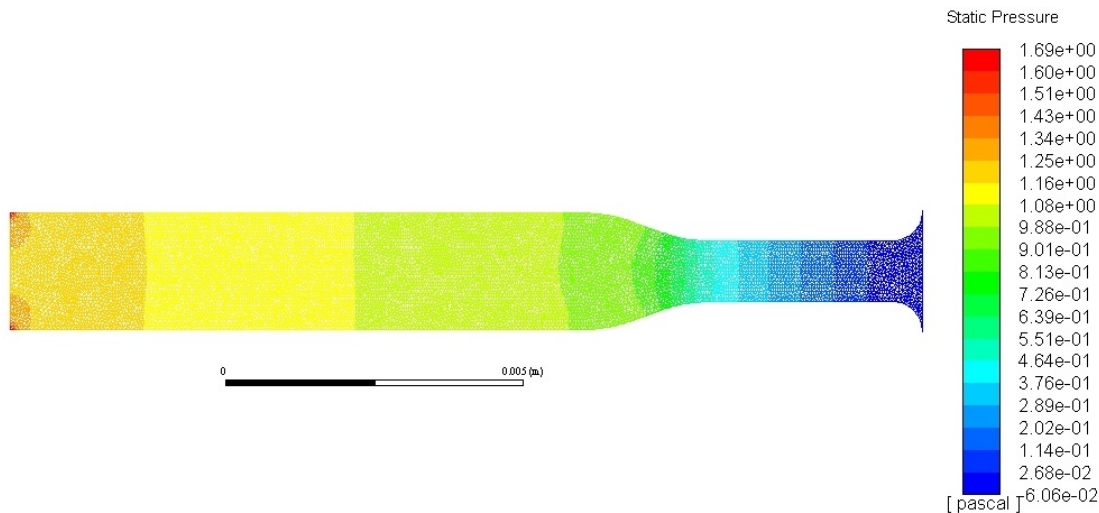


FIGURE 6.8: Pressure Drop Evaluation with FLUENT®.

6.5.1 Old Equipment and Laboratory Activities

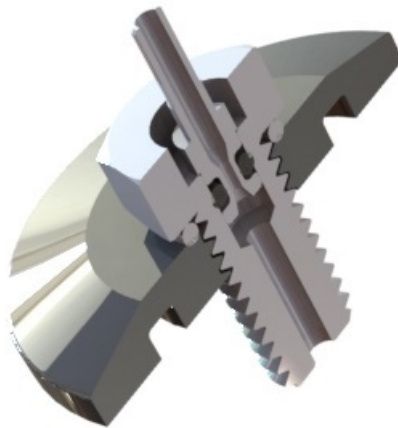


FIGURE 6.9: Old Test Equipment.

The first equipment tested is presented in Figure 6.9¹⁷, the insert is pushed in a sealing screw connected with a flange.

The small vacuum vessel in the Clean Room A of Lab 3 can be easily equipped with standard KF-25 flanges, so we decide to thread one of them and to use a sealing screw machined too in order to reproduce the gland geometry.

Once the parts arrived from the Machine Shop they were firstly measured then the free end of the insert was filled with epoxy (Figure 6.10). The idea was to ensure that the only possibility to leak was through the OR and to low the backgrounds as much as possible.

The parts were cleaned with alcohol and some grease was used with the ORs (Figure 6.11) then the parts were assembled and mounted on the vacuum vessel (Figure 6.12).

After several run and different configurations was clear that the backgrounds, mainly

¹⁷For the mechanical drawings please refer to Appendix C.

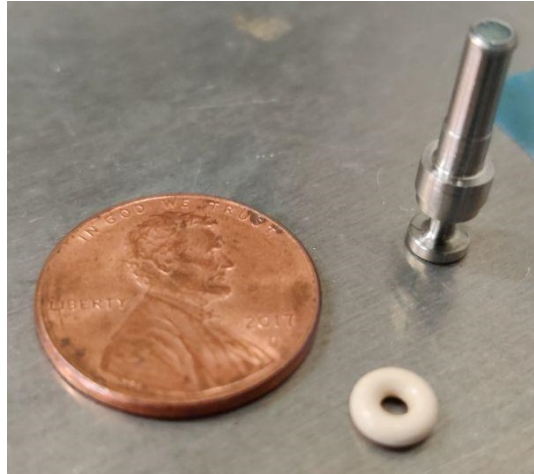


FIGURE 6.10: Insert machined and plugged with epoxy (with the OR and a coin of one cent).

consisting of the bigger OR of the sealing screw, where to high to obtain good data in this way.

6.5.2 New Equipment

The new idea suggest by my Supervisor Mete Yucel was to continue to use a standard flange but thicker than the previous one¹⁸.

In this second experiment the equipment is in the vacuum chamber and the inlet and the outlet are connected with the outer through the flange.

6.6 Conclusion

With the second equipment my Supervisors reached the pressure required and collected data. The result is that:

- The background is 0.0043sccm +/- 0.001sccm;
- The equipment with six Gas Connectors showed 0.0046sccm +/- 0.001sccm.

The amount for each connector is about $5 * 10^{-5} sccm$ then the total is 0.0216sccm¹⁹, in relative terms is the 0.36% of the total Tracker leak budget. The connectors met all the requirements and can be used in the final Tracker design if the interfaces will provide the correct finishing required.

¹⁸The last parts ordered were a standard Flange Cap (its mechanical drawing can be find in Appendix C) with its copper gasket.

¹⁹It's worth to remember that we have 216 lines on the inlet and the same number for the outlet then the total number of the connectors is 432.



FIGURE 6.11: Parts Ready for the Test.

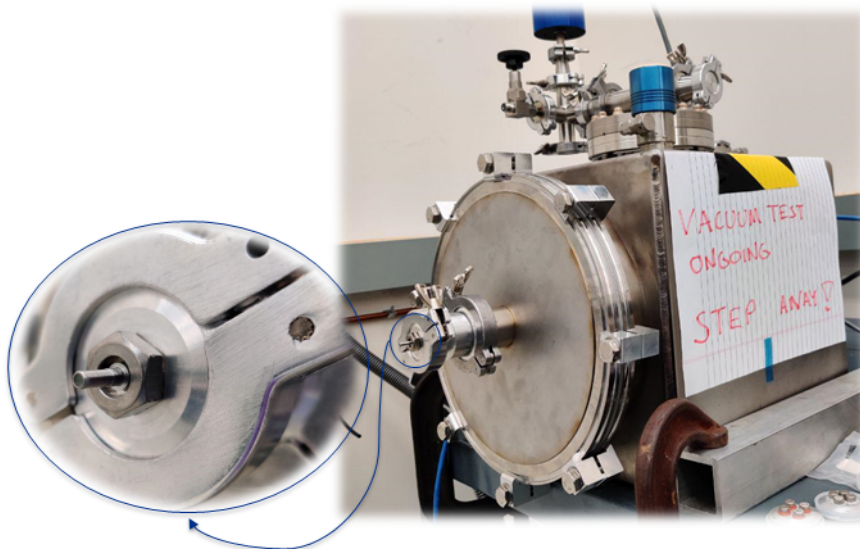


FIGURE 6.12: Equipment Mounted on the Vacuum Chamber.

Chapter 7

Interfaces

7.1 A Short Overview

The Interfaces are the only aspect that is still missing. As already said in Sub-Section 4.1.3 they are conceived to be the trait d'union between the Printed Part and the remaining elements. The current Connector' solution stated that we have only two chances to design the interface on the Calorimeter side¹.

- The first chance is that the Printed Part itself can provide the correct surface finishing or be machined to reach it;
- The second chance is that a new part must be used.

The main issue connected with a new part is that must be linked to the Printed Part. Since that the surface is wide and 216 holes quite close one to each other are machined in it, this operation appears difficult to be completed with the requested reliability.

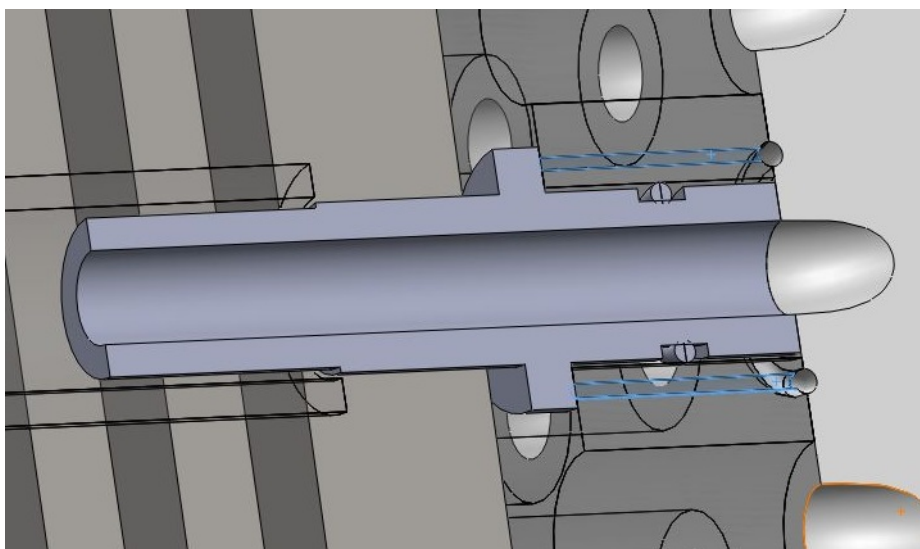


FIGURE 7.1: Suggestion for a Stand-alone Interface.

Figure 7.1 showed a suggestion for a stand-alone interface. A toroidal channel is machined between the two parts, then two or more small holes allow to fill the above mentioned toroid with resin. The clear material can simplify the detection of bubbles or not complete filling.

¹The epoxy connection on the Tracker side doesn't require any further considerations.

Chapter 8

Blocking System

The aim of the Blocking System is to avoid the pull-out of the connectors by the pressure. The design was basically conceived in the last days of the program and it's currently under review.

It is made up of two main elements that are:

- The external structure;
- The comb-like part.

8.1 External Structure

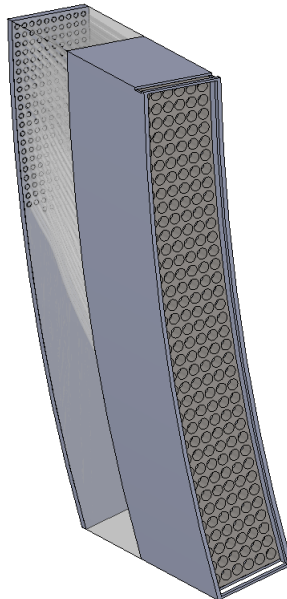


FIGURE 8.1: External Structure Mounted on the Printed Part.

The external structure has a uniform thickness of 1mm and it's placed where I started to save more space on the outer surface of the Printed Part¹. The main task is to provide a seat for the comb-like part, for this reason it is milled on the internal surfaces along the radial direction where it has two different openings.

¹For more details please refers to Sub-Section 5.2.2.

8.2 Comb

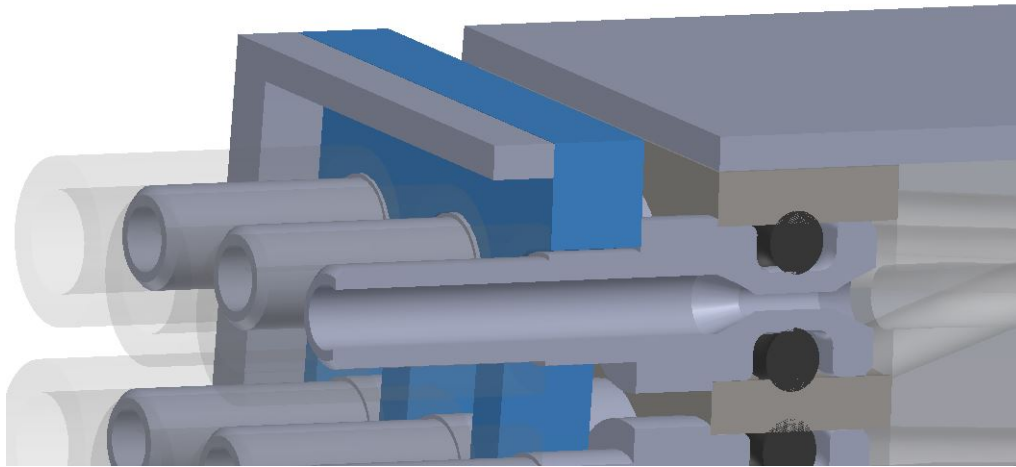


FIGURE 8.2: Blocking System: How the comb hold the connectors.

The Comb² is positioned between the Interface and the External Structure. It's the element that transfer the actions from the connectors to the External Structure. An overview of the assembly operations made with Solidworks can be found at [SolidWorks Assembly A. Fino](#).

²The blue one in Figure 8.2.

Appendix A

Non Standard off the shelf OR formulas

Although the chosen OR is the standard one, some evaluations were performed to make a comparison between the two choices. As already stated in Chapter 6.3 some useful data are re-listed and some other else are defined¹:

$$stretch_{min} = 0.01$$

$$stretch_{max} = 0.05$$

$$min_{OR_compression} = 0.1$$

$$max_{OR_compression} = 0.4$$

$$\phi_{bore_nominal} = 4.26mm^2$$

$$\phi_{bore_tolerance} = 0.026mm^3$$

$$\phi_{OR_CS_tolerance} = 0.08mm$$

$$\phi_{OR_ID_tolerance} = 0.13mm$$

$$\phi_{piston_tolerance} = 0.03mm^4$$

With the hypothesis of simmetrical tolerance:

$$\phi_{bore_min} = \phi_{bore_nominal} - \phi_{bore_tolerance}$$

$$\phi_{bore_max} = \phi_{bore_nominal} + \phi_{bore_tolerance}$$

$$\phi_{OR_ID_min}(\phi_{OR_ID_nominal}) = \phi_{OR_ID_nominal} - \phi_{OR_ID_tolerance}$$

$$\phi_{OR_ID_max}(\phi_{OR_ID_nominal}) = \phi_{OR_ID_nominal} + \phi_{OR_ID_tolerance}$$

We can define the piston ID as function of the stretch factor (see Chapter 6.3):

$$\phi_{piston_max}(\phi_{OR_ID_nominal}) = \phi_{OR_ID_min}(\phi_{OR_ID_nominal}) * (1 + stretch_{max})$$

$$\phi_{piston_min}(\phi_{OR_ID_nominal}) = \phi_{OR_ID_max}(\phi_{OR_ID_nominal}) * (1 + stretch_{min})$$

We have all the elements to draw the lower and upper lines:

$$CS_{OR_max}(\phi_{OR_ID_nominal}) = \frac{\phi_{bore_min} - \phi_{piston_max}(\phi_{OR_ID_nominal})}{1 - max_{OR_compression}} - \phi_{OR_CS_tolerance}$$

$$CS_{OR_min}(\phi_{OR_ID_nominal}) = \frac{\phi_{bore_max} - \phi_{piston_min}(\phi_{OR_ID_nominal})}{1 - min_{OR_compression}} + \phi_{OR_CS_tolerance}$$

¹The data strictly connected with the geometry are not general and supplied by the specific seller please check yours.

²This value was chosen in order to have a clearance of 1mm.

³This value is connected with a particular bushing chosen from a well known Fermilab' supplier.

⁴Assuming an IT6 and that the diameter is always less than 3mm.

Appendix B

Pressure Drop Evaluation

The following calculations were performed with a Mathcad® sheet and were used to have an overestimation of the losses through the connector.

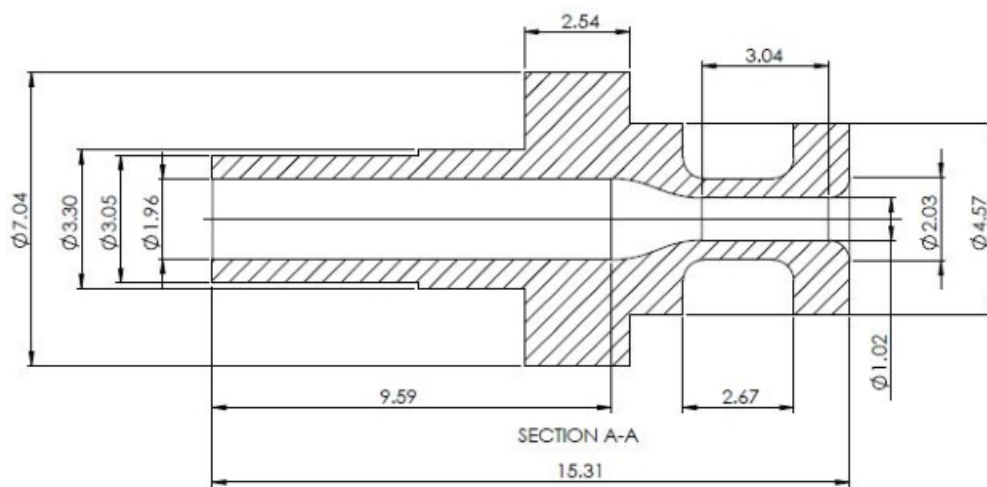


FIGURE B.1: Connector Geometry used for the Pressure Drop Evaluation.

Let's start defining some geometric dimensions:

- Length of the cavity with the bigger hole: $l_1 = 9.6\text{mm}$;
- Length of the cavity with the smaller hole: $l_2 = 3.04\text{mm}$;
- Wall thickness: $s_{\text{wall_tick}} = 0.5\text{mm}$;
- AS568-004 ID: $\phi_{\text{AS568_004_ID}} = 1.956\text{mm}$;
- OD of the piston: $\phi_{\text{OD}} = \phi_{\text{AS568_004_ID}}$;
- ID of the piston: $\phi_{\text{ID}} = \phi_{\text{OD}} - 2 * s_{\text{wall_tick}}$;
- The radius of the bigger hole is: $r_{\text{hole}} = \frac{1.96}{2}\text{mm}$;
- The radius of the smaller hole is: $r_2 = 0.5\text{mm}$;
- The flow-rate is $\Phi_{\text{flow_rate}} = 9.6 * 10^{-7} \frac{\text{m}^3}{\text{s}}$;
- The density of the gas-mix is: $\rho_{\text{mix}} = 0.2 * \rho_{\text{CO}_2} + 0.8 * \rho_{\text{Ar}} = 1.785 \frac{\text{kg}}{\text{m}^3}$ ¹;

¹The two densities are evaluated using Refprop® with the pressure equal to 0.11MPa and the Temperature equal to 25°C.

- The kinematic viscosity of the gas-mix is: $\mu_{mix} = 0.2 * \mu_{CO_2} + 0.8 * \mu_{Ar} = 2.106 * 10^{-5} \frac{kg}{m*s}$.

The speed can be retrieved from the flow-rate formulas, then using the Reynold's number definition we can find that:

- $Re_1 = 52.855$;
- $Re_2 = 103.596$.

For both the parts the flow is laminar, so we can use an approximation of the friction's coefficient²:

- $f = \frac{64}{Re}$.

The formulas for the distributed losses used is³:

- $\Delta p_{distributed} = f * \frac{l}{d} * \frac{\omega^2}{2*g} * \rho_{mix}$.

There're also two concentrated losses connected with the variation of diameter, to be conservative the transitions will be modelled as abrupt changes:

- $R_{2_1} = [1 - (\frac{r_2}{r_{hole}})^2]^2 = 0.547$;
- $C_{1_2} = 0.582 + (\frac{0.0418}{1.1 - \frac{r_2}{r_{hole}}})$;
- $R_{2_1} = (\frac{1}{C_{1_2}} - 1)^2 = 0.283$;
- $\Delta p_{concentrated} = f * \frac{R*\omega^2}{2*g}$.

The result is: $\Delta p_{tot} = \Delta p_{concentrated_{1-2}} + \Delta p_{concentrated_{2-1}} + \Delta p_{distributed} = 4.146Pa$

²This approximation is good enough until Re=2000.

³This is the Darcy's formulas

Appendix C

Mechanical Drawings

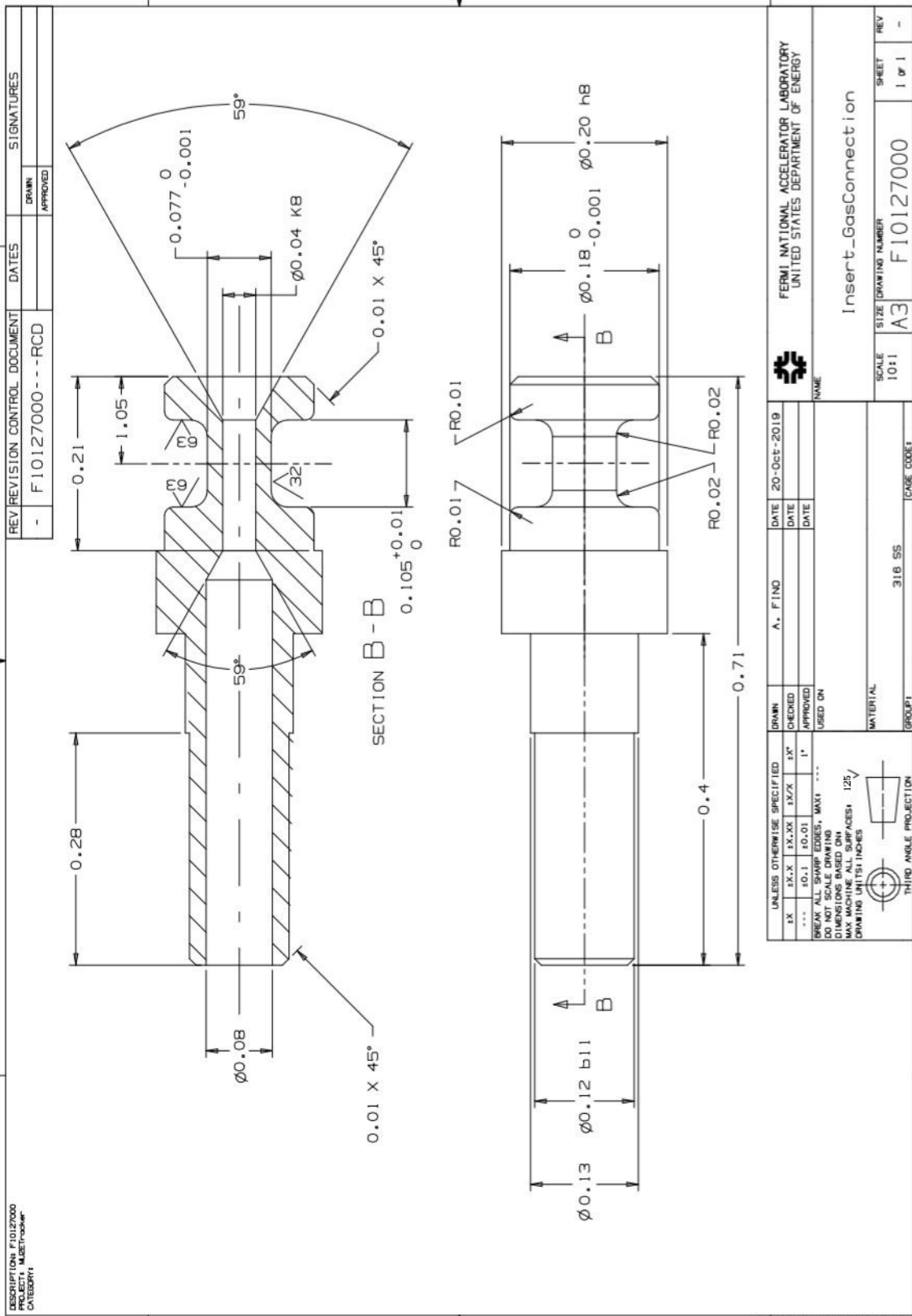


FIGURE C.1: Insert, Mechanical Drawing.

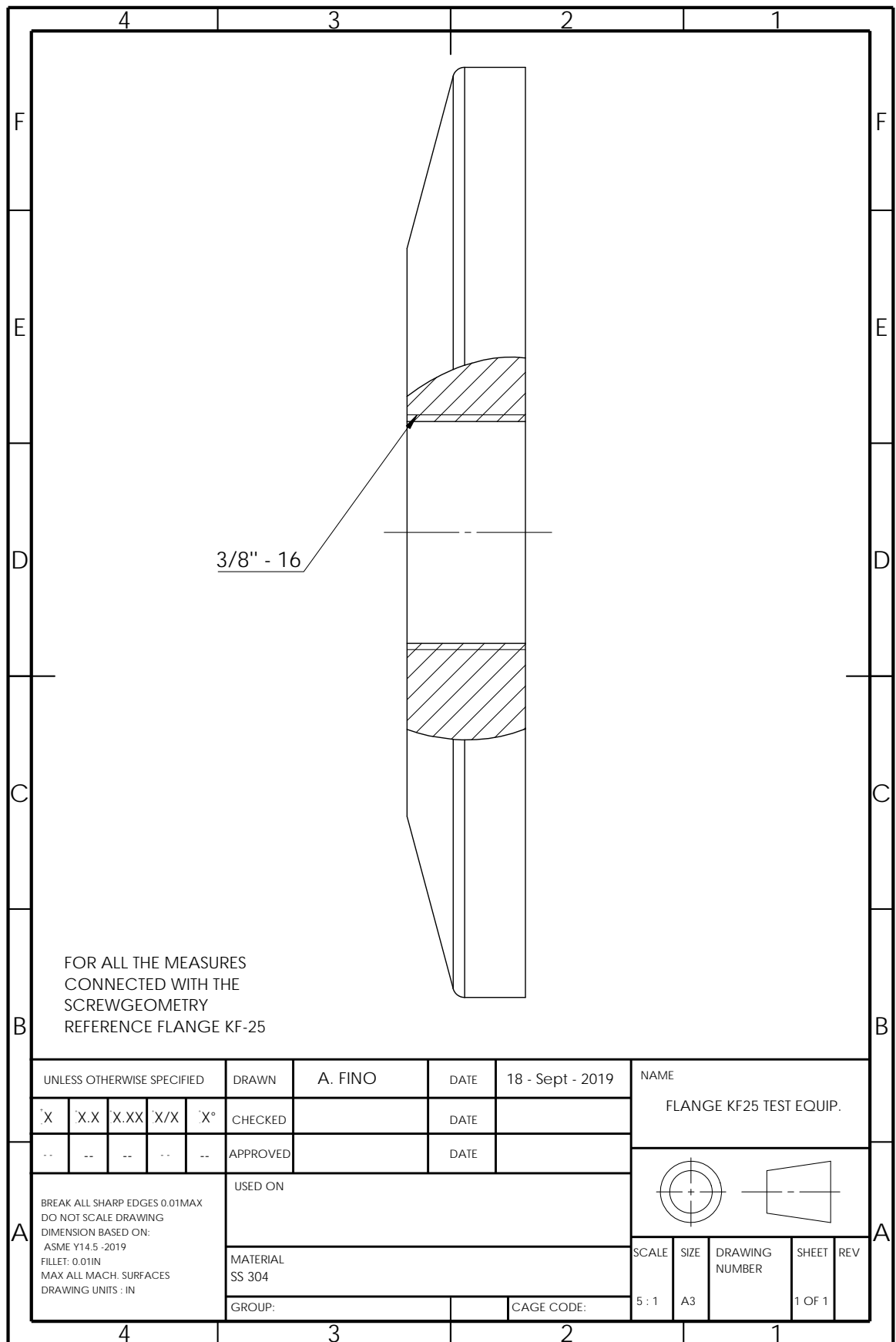


FIGURE C.2: KF Flange Modified, Mechanical Drawing.

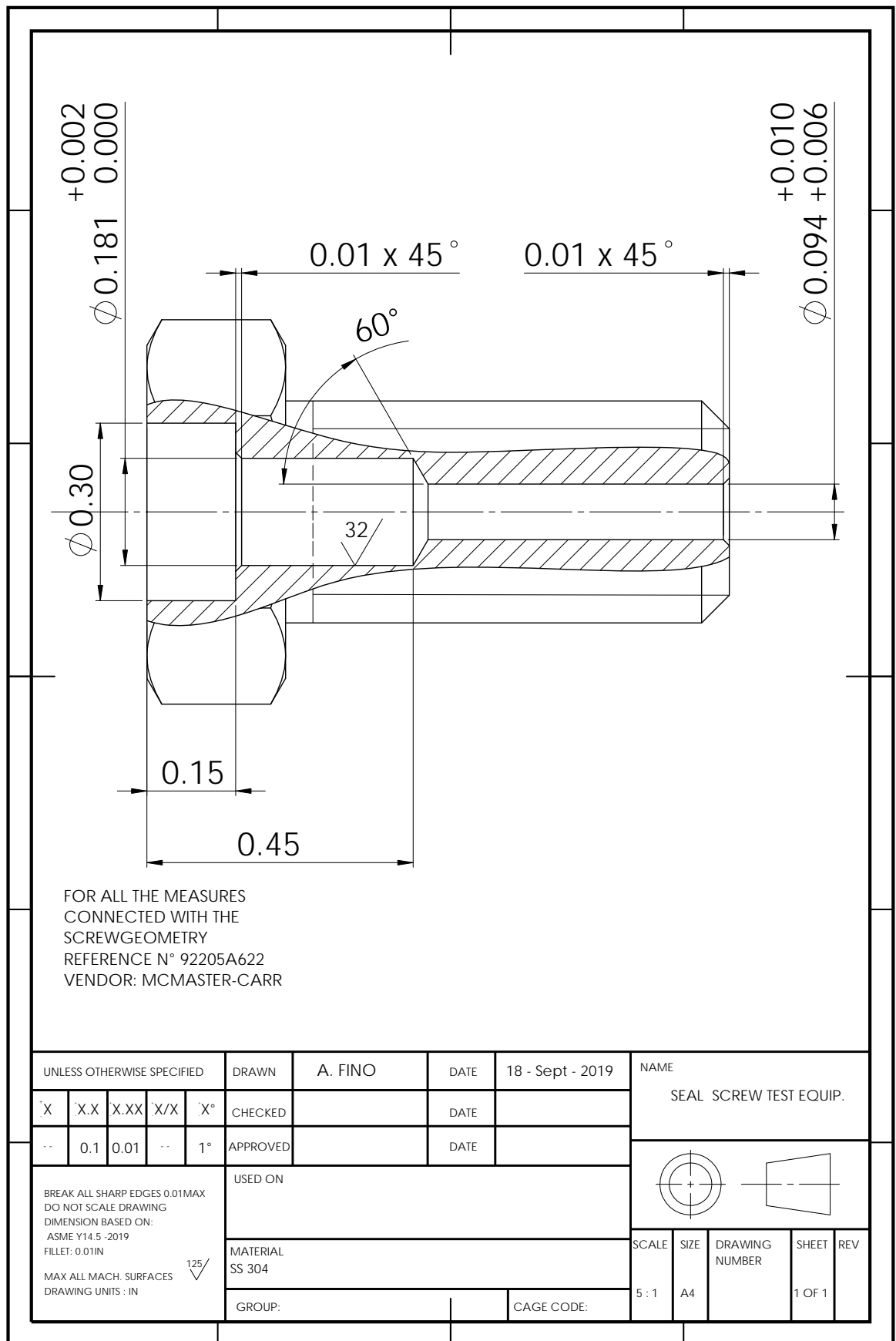


FIGURE C.3: Sealing Screw Modified, Mechanical Drawing.

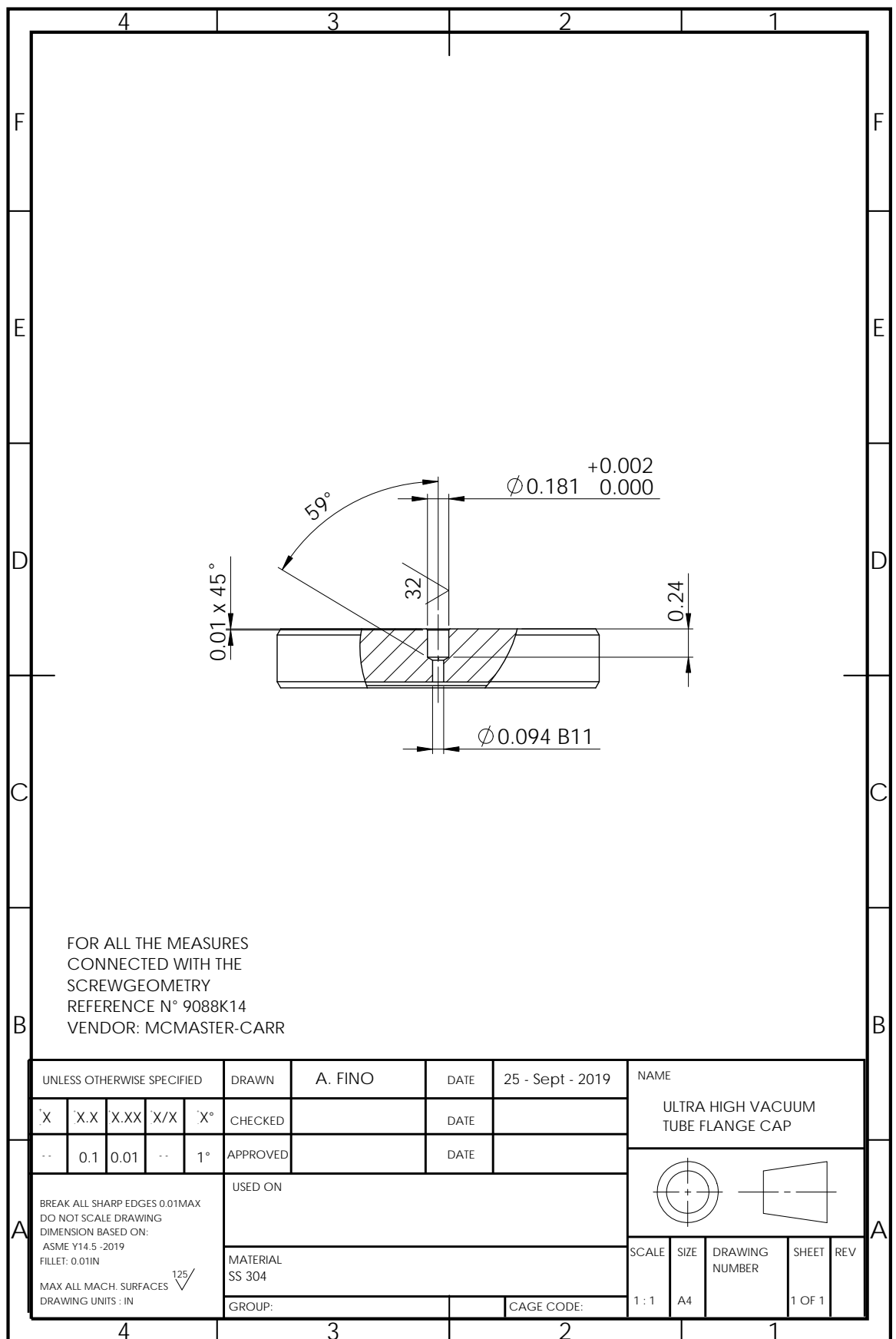


FIGURE C.4: CF Modified, Mechanical Drawing.

Appendix D

Bibliography

- Mu2e-docdb-732 – Tracker Requirements Document – R. H. Bernstein, A. Mukherjee [1]
 Perspective 28 Jan 2019 doi: 10.3389/fphy.2019.00001 – The Mu2e Experiment – R. H. Bernstein [2]
 PASCOS 2016 XIIth Rencontres du Vietnam, ICISE, quy Nhon, Vietnam – Charged Lepton Flavor Violation: An Overview – R. Bernstein [3]
<https://en.wikipedia.org/wiki/Mu2e> – Mu2e – Wikipedia [4]
<https://mu2e.fnal.gov/> – Mu2e: muon-to-electron-conversion experiment – FNAL [5]
 Mu2e Technical Design Report October 2014 – Fermi National Accelerator Laboratory [6]
 Mu2e JPARC Symposium2019 V3 – Mu2e at Fermilab – R. Ray [7]
 T-Tracker Geometry 16 Nov 2017 – A. Mukherjee [8]
 Mu2e-docdb 4991-v4, April 2016 – Tracker Layout – G.Gallo [9]
 Mu2e-docdb 27691-v1 22 Jul 2019 – Weekly Tracker’s Meeting - M. Yucel [10]
 Mu2e docdb 25017-v2 22 Mar 2019 – Weekly Tracker’s Meeting - M. Yucel [11]
 Mu2e docdb 1383-v7 7 Mar 2011 – Requirements and Specifications for WBS 5.10 - Detector Support and Installation System – R. Bossert [12]
 Mu2e docdb 28426-v1 10 Sep 2019 – Tracker’s Gas Connection updates – A. Fino [13]
 Mu2e docdb 28429-v1 10 Sep 2019 – Tracker’s Gas Connection [printed_part] – A. Fino [14]
 Mu2e docdb 28758-v1-v1 10 Sep 2019 – Tracker’s Gas Connection updates – A. Fino [15]
www.applerubber.com – Apple-Seal Design Guide – Apple Rubber Products [16]
 IEEE Transactions on Nuclear Science, Vol. NS-32, No. 5, October 1985 – Radiation Resistance of Elastomers – G. Lee [17]
 Mu2e-docdb 29523-v2 25 Oct 2019 – Tracker Panel Tests - Vacuum and Pressure – M. Yucel [18]